ARTICLE TITLE

T2* Mapping Techniques: Iron Overload Assessment and Other Potential Clinical Applications

AUTHOR NAMES AND DEGREES

Katia Menacho, MD

Amna Abdel-Gadir, MBSS

James C Moon, MB, BCh, MRCP, MD

Juliano Lara Fernandes, MD, PhD, MBA

AUTHOR AFFILIATIONS

KM - Barts Heart Centre, The Cardiovascular Magnetic Resonance Imaging Unit and Institute of Cardiovascular Science, University College London, London, UK.

AAG - Institute of Cardiovascular Science, University College London, London, UK

JLF – Jose Michel Kalaf Research Insitute, Radiologia Clinica de Campinas, Campinas, Brazil

JCM - Barts Heart Centre, The Cardiovascular Magnetic Resonance Imaging Unit and The Inherited Cardiovascular Diseases Unit, St Bartholomew's Hospital, West Smithfield, London, UK.

AUTHOR CONTACT INFORMATION

KM – Barts Heart Centre, St Bartholomew's Hospital, 2nd Floor, King George V Block, London EC1A 7BE, United Kingdom. katia.menacho.m@upch.pe

AAG – Barts Heart Centre, St Bartholomew's Hospital, 2nd Floor, King George V Block, London EC1A 7BE, United Kingdom. amnagadir@yahoo.co.uk

JLF – Av Jose de Souza Campos 840, Campinas, SP, 13092-100, Brazil. jlaraf@terra.com.br

JCM - Barts Heart Centre, St Bartholomew's Hospital, 2nd Floor, King George V Block, London EC1A 7BE, United Kingdom. james.moon@bartshealth.nhs.uk

CORRESPONDING AUTHOR

JLF – Jose Michel Kalaf Research Insitute, Radiologia Clinica de Campinas, Campinas, Brazil. Av Jose de Souza Campos 840, Campinas, SP, 13092-100, Brazil. jlaraf@terra.com.br

DISCLOSURE STATEMENT

No conflict of interest.

KEYWORDS

Parametric mapping, T2*, iron overload, blood oxygen level dependent (BOLD), hemorrhage

KEY POINTS

1. T2* mapping sequences are widely accessible in most commercial scanners and multiple tools to quantify it are available.

2. New technical developments have made possible automated and free-breathing acquisition of T2* maps with no major limitations on age.

3. Routine T2* assessment of iron overload is recommended in patients with chronic transfusions and have significantly changed prognosis and treatment strategies.

4. T1 and T2 maps can be used for iron overload assessment and evidence is rapidly increasing for these alternative methods in this scenario.

5. Intramyocardial hemorrhage, microvascular obstruction and blood oxygen level ischemia assessment are important variables in acute and chronic CAD that can be evaluated with T2* maps.

SYNOPSIS

T2* mapping techniques has evolved significantly since its introduction in the early 2000s and a significant amount of evidence has been gathered to support its clinical routine use for iron overload assessment. This review focuses on the most important aspects of how to perform T2* imaging, from acquisition, to post-processing to analyzing the data with clinical concentration. Newer techniques have made T2* mapping more robust and accurate, allowing for a broader use of this technique for non-contrast ischemia imaging based on blood oxygen levels, in addition to evaluation of intramyocardial hemorrhage and microvascular obstruction.

Multi-parametric mapping of the myocardium has become an area of great interest in the recent year with multiple review papers and recommendation statements.[1] Despite most of the focus initially on T1 mapping and then on T2/edema imaging, T2* mapping was the first clinically useful parametric mapping technique for the heart.[2] Before the introduction of T2* as a diagnostic tool, iron induced cardiomyopathy was the most common cause of death in transfusion dependent thalassemic patients. It has been now more than 18 years since the initial applications of T2* images in iron overload assessment began to be performed and the accumulated knowledge gained from that has led to important practical changes in the diagnosis and treatment with chelation. T2* is the current method of choice for the assessment of cardiac iron deposition, with proved evidence in reduction of overall mortality (improvement on life expectancy and less cardiovascular complications on transfusion dependent patients). Moreover, faster protocols can make this technology available in developing countries. In this review, we summarize the most important aspects of T2* mapping when applied in clinical practice, with an additional look into other applications where T2* maps might also provide unique important data beyond traditional clinical and imaging markers.

T2* techniques: from acquisition to post-processing

Physical Parameter: T2* imaging

T2* represents the decay of transverse magnetization due to a loss of coherence between spins and magnetic field inhomogeneity.[3] This relaxation is measured using gradient echo (GRE) imaging. This transverse relaxation is eliminated when a 180-degree pulse is applied using a spin echo

sequence (SE - true T2 relaxation) which removes the magnetic field inhomogeneity,[4] as illustrated in Figure 1. The principle of T2* relaxation is involved in numerous MR applications with GRE sequences such as perfusion techniques and functional imaging sequences.

T2* imaging to assess iron loading

A fundamental principle to generate images for iron quantification is by applying a strong magnetic field and radiofrequency signals through GRE sequences, with time of decay controlled by the MRI scanner. The longer the echo time (TE) the darker the resultant image; iron-mediated darkening can be characterized by a half-time constant and is non-linearly proportional to the level of iron concentrations. Often, this darkening is described as a rate principle (R2*) rather than a time constant. The relaxation rate is just the reciprocal of the time constant, R2* = 1000/T2*. The factor of 1000 is included because T2* is expressed in milliseconds (ms) and relation rates in expressed in Hertz (sec^{-1}).[5, 6] To calculate T2*, an application of multiple radio frequency pulses leads to the generation of a series of images with different echo times (ET).[7]

Traditional sequences to measure cardiac iron overload

Most updated international expert consensus suggest that for T2* cardiac iron loading assessment, a multi-echo gradient echo with eight equally ranging from 2 to 18ms may be used o on a 1.5T MRI scanner.[1] Fat saturation is needed for the liver, but is not essential for heart images. Good shimming of the heart is a requirement for accurate measurements and manual volume shimming may be required in order to reduce potential artifacts. Once adjusting these factors, both bright blood and dark blood techniques are validated and widely used clinically.[8,9]

-*Bright blood technique*:[8] images are acquired immediately after the R wave to reduce artifacts caused by blood flow and myocardial wall motion.[4]

-*Dark blood technique*: a double inversion recovery pulse is used to null the signal from blood; multiecho T2* acquisition is extended to late diastole with minimal cardiac motions technique.[10] Compared to bright blood technique, dark blood has shown to have superior reproducibility, less artifact susceptibility and it is the preferred method to use clinically (Figure 2).[10,9]

Post-processing and myocardial T2* calculation

The measurement of myocardium iron is typically performed in a mid-ventricular short axis image.[4, 10] The septal iron concentration largely reflects the global iron content as shown in biopsy studies,[1, 11] so analysis can be restricted to this segment to avoid artifacts due to susceptibility effects (Figure 3).

One of the most important limitations for post-processing is the signal plateau, which complicates the approach to the curve fitting method for evaluation the T2*.[12] Different approaches have been designed to tackle this. The truncation model discards the late "plateau" points and then the remaining signal is fitted with a monoexponential equation.[13] The other common method is the offset model, in which an exponential equation plus a constant offset is used to tackle this problem.[7] As a general perspective, the use of offset models may produce underestimation of T2* values on bright-blood data, making it less reproducible when comparing with truncation method (Figure 4).[12]

Several approaches are trying to improve truncation model accuracy, especially in severe iron stages, where artifact produces major limitations. Nonlocal means (NLM) providing more accurate pixel-by-pixel MRI relaxometry may improve tissue characterization.[14] Moreover, a noise-

corrected model has been created, limiting analysis to the region of interest (ROI-base curve fitting) and consistently producing accurate and precise R2* values by correctly assessing the non-central chi noise.[15] Most clinical vendors and dedicated cardiovascular software have validated methods of interpreting T2* data with both FDA and CE-approval.[16-19] Open-source software are also available and validated against commercial tools[20-23] resulting in a large number of options for sites to choose from in order to quantify T2* with high accuracy.

Breath hold versus free breathing techniques

Pixel-wise mapping techniques involves curve fitting on individual pixels; it offers a more spatial context than ROI-based methods for the delineation of adjacent tissues with different tissue values[24] and therefore, provides a surrogate measure of the iron distribution.[7, 25-27] This technique covers the entire field of view and provides important information to identify artifacts that may be less apparent. Moreover, pixel-wise mapping is automatic, reduces time of analysis[28] and the median values calculated from partial interventricular septum region provide lower intra- and inter-observer variabilities compared with conventional technique.[29] However, the main limitation with breath-held mapping is noise and the possibility of artifacts due to the relatively long breath-hold times. As an alternative, a free-breathing T2* mapping method was developed with full automation, truncation of long echo time and low SNR images after motion correction with highly accelerated multi-GRE acquisition and multiple averages to improve SNR. This method resulted in consistently good quality maps, especially when respiratory motion and arrhythmias are present and with same time of acquisition as breath-hold techniques.[28] Other free-breathing methods also demonstrated accurate results in the heart, with improved temporal resolution using single-shot gradient-echo echo-planar imaging (GRE – EPI) enabling accurate myocardial measurement and

being insensitive to respiratory motion.[30] Figure 5 demonstrates examples of different imaging techniques, including breath-hold and free-breathing approaches.

Clinical application of iron overload assessment with T2*

Since its introduction in early 2001, the use of T2* imaging to guide therapy in patients with iron overload, coupled with improvement in chelator options and advances in other coadjuvant management strategies, resulted in significant reduction in cardiovascular death and disability in thalassemia major patients.[31, 32] T2*CMR is a recommended exam in practically all clinical guidelines relating to iron overload treatment[33-35] and its use has been summarized in specific recommendation statements as well.[36]

From a practical standpoint, transfusion dependent patients should start monitoring myocardial T2* at the age of 10 years old if they are routinely followed and have a history of being well chelated.[37] However, patients in whom the treatment follow-up is unclear, have irregular chelation or very high liver iron concentrations (LIC), may perform their first MRI scan at ages as early as 7 years old as significant myocardial iron concentrations (MIC) have been described at this early age.[38] While initial T2* techniques performed poorly in very young children due to lack of breath holding or movement, the newer free-breathing technique cope with these difficulties fairly easily and provide very good quality images, making age restrictions not a limitation to when to begin scanning patients anymore as shown in Figure 6.

Once started, routine follow-up of myocardial iron concentrations should be performed yearly in most patients, with this interval varying from 6 months to 2 years depending on specific clinical conditions and service availability.[39] It is important to note that removal of cardiac iron in the heart is a relatively slow process and specially in acute settings (i.e. acute heart failure) the clinical condition will sometimes improve significantly while T2* changes will not be proportional.[40] The main reason for this disparity is that T2* is measuring mostly chronically stored iron in lysosomes while the iron being mobilized by intensive chelation is in labile form, with little T2* effects.[36] Nevertheless, monitoring the effects of iron chelation or accumulation is a primary target of routine MRI scans in these patients and any changes above the coefficient of variation of 4% for black blood images and 8% for bright blood images should be considered significant changes.[41]

Another important clinical aspect of using T2* for iron overload assessment involves the correlation of T2* values and MIC. While for the liver, at a very early stage in the development of the technique, T2* values and LIC correlations were established, for the heart T2* was the main variable used for quantification until Carpenter et al performed the comparison of this MRI value to MIC measured biopsied hearts.[11] As T2* and MIC are not linearly related, one must take this into account when assessing longitudinal changes in T2* values as significant changes in MIC occur when small variations are seen at low T2* values. The correlation of T2* and MIC can be seen in Figure 7 using the equation $MIC = 45 \times T2^{*-1.21}$ as published by Carpenter et al.[11]

When reporting the iron concentrations obtained with various T2* techniques, the value of 20ms has been traditionally associated with the normal cutoff for non-iron overloaded myocardial

tissue based on the initial Anderson et al data that showed that almost all patients with T2* above these levels did not develop reductions in left ventricular ejection fraction.[2] However, despite the popularity of this number, other authors have shown that iron deposition is frequently found in patients with septal T2* above these levels.[42] Therefore, it would be more appropriate to consider the normal myocardial T2* levels according to measurements performed in normal volunteers where normality was established at 36.1 ± 4.5 ms.[43] Nevertheless, traditional reporting tables for iron overload using T2* have used cutoffs based on clinical management strategies and prognostic data. Table 1 lists the values of myocardial T2*, MIC and the reporting levels for iron overload in the heart. It is important to note that although a T2* levels <10ms is considered severe, risk elevates dramatically as T2* falls further from 10 to 8 to 6 and even 4ms.[44] As for normal values, correlations with T1 suggest that 26ms would be a more appropriate cut-point for T2*, and several centers worldwide report potential early iron in the 20-26ms range.[45] While not the focus of this review, we have also included the corresponding liver reference values as usually both measurements are performed in the same patient with the corresponding calibration curves.[46] A more thorough review of liver iron concentration measurements can be found elsewhere.[39] Despite the fact that the main recommendations for iron overload assessment generally are performed at 1.5T, many studies have now also performed correlations of iron overload at 3T and these values are reported in Table 1 as well using one of the reference studies with this field strength.[47]

Alternative Methods and comparisons (T1 and T2 mapping)

As demonstrated in the previous paragraphs, the CMR T2* parameter has transformed the management of patients with iron loading conditions allowing robust, non-invasive quantification of myocardial iron.[2] It provides tailored and personalized approaches to chelator dosing which has been linked to improved survival.[31] To further improve diagnostic accuracy there has been a rising interest in alternative MRI methods in the way of native (non-contrast) T1 and T2 mapping to aid the diagnosis of myocardial iron in patients with equivocal disease. Ferritin and hemosiderin alter the behavior and properties of hydrogen nuclei in water within tissue shortening both T1 and T2 times, similar to T2*. The adoption of CMR parametric mapping techniques in the diagnosis of myocardial diseases, including cardiac amyloidosis and Fabry disease, has been supported by the SCMR Consensus Statement[1] and reflected in the development of commercially available mapping sequences by all major CMR scanner manufacturers. Mapping sequences allow the measurement and display of relaxation times in color on a pixel-by-pixel basis without the need for complex post-processing.[48-51] For the measurement of myocardial iron using T1 and T2 mapping, like with T2*, a region of interest is recommended in the interventricular septum using a short axis slice.[1] Indeed, by removing complex analysis, abbreviated mapping protocols can be performed as it was shown by Abdel-Gadir et al who performed non-contrast CMR for iron overload in Bangkok in 8 minutes per exam, 50 patients/day on one magnet, reducing costs four-fold and demonstrating the clinical and economic advantages.[52]

T1 mapping for iron

T1 is an intrinsic magnetic property that represents longitudinal recovery time after excitation of hydrogen atoms. At selected magnetic field strengths, each tissue has its own characteristic range of values, and deviation from these values implies disease. T1 values are increased with the expansion of the extracellular compartment by fibrosis, edema and amyloid, and reduced in iron, lipid accumulation, and haemorrhage.[53] T2* is more specific and really only influenced by the presence of iron – although unrecognized use of gadolinium contrast agent may reduce T2*. In the liver, one case report has demonstrated cobalt-chromium from a degenerating metal-on-metal hip as reducing T2*.[54] T1 mapping was first introduced using the inversion recovery based modified look-locker imaging sequence (MOLLI), with further developments including the shortened MOLLI (ShMOLLI) which requires an acquisition time over nine heartbeats.[49, 50] Newer sequences including saturation recovery single-shot acquisition (SASHA) and saturation pulse prepared heart-rate independent inversion recovery (SAPPHIRE) yield higher accuracy, lower precision and similar reproducibility compared with MOLLI and ShMOLLI.[51, 55] This however means that different sequences have differing normal ranges. This is less important than it sounds as tissue iron, if present, dominates measured T1 – falls in T1 of up to 20 standard deviations have been reported with severe myocardial iron.

The role of T1 mapping in the detection of iron has been promising to date at both 1.5T and 3T, and has been shown to correlate with cardiac iron in vitro.[56] Early data by Sado et al was the first to demonstrate that myocardial T1 mapping has excellent reproducibility and correlates well with T2* in a group of 88 patients with suspected iron overload.[57] Using the ShMOLLI sequence, T2* was lower in patients than healthy volunteers (836± 138ms versus 968 ± 32ms, $p < 0.0001$), and no patient with a low T2* value had normal T1 values. This study also demonstrated

superior interstudy reproducibility of T1, particularly when low levels of iron are present, and reclassified a significant proportion of patient as having mild cardiac siderosis, doubling the number of patients identified with iron, although almost all of this is mild. These findings were further explored in larger international studies using different T1 mapping sequences.[45, 58] A key unknown question is whether using T1 mapping would detect changes in iron loading better than T2* for individual patients (smallest detectable difference) or in studies (increased power). An example and comparison of myocardial T1 images to T2* is shown in Figure 5.

The rise in clinical use of 3T scanners for non-cardiac conditions may provide diagnostic challenges for patients requiring iron quantification as T2* mapping is not routinely recommended at 3T. The second mapping consensus statement specifically recommends that T2* mapping for iron overload currently should be performed at 1.5T only.[1] T1 mapping may however be used as a method to quantify iron at 3T where T2* measurements are not possible.[59] Alam et al demonstrated the feasibility of T1 at both 1.5T and 3T, and its superiority to T2* when assessing reproducibility.[59]

The administration of contrast and acquisition of a post-contrast T1 map allows the generation of an extracellular volume (ECV) map wherein pixel values represent the interstitial volume. In a small single center study, ECV was increased in patients with thalassemia major with prior myocardial iron overload, whilst patients without historical iron loading had no evidence of increased ECV. The association between iron and ECV remained significant after controlling for patient age, gender, and cardiovascular risk factors.[60]

Despite the advantages of T1 mapping as a complementary diagnostic tool there are challenges facing its clinical utilization. There is a known variation of absolute T1 values between sequences and scanners, and it is susceptible to alteration in a large number of diseases of the

heart muscle.[61] Nevertheless, T1 appears to be a more precise measurement of myocardial iron.[45, 57, 58]

T2 mapping for iron

T2 relaxation time reflects the time for the MR signal to decay in the transverse plane, and is commonly used to assess myocardial inflammation and oedema.[1] As with T1 and T2*, iron deposition in the myocardium causes shortened T2 values. Very little work is available in the literature on the use of T2 for the diagnosis of myocardial iron loading. In a 200 thalassemia patient study in Thailand, at 1.5T T2 mapping correlated strongly with T2* in patients with myocardial iron loading ($r= 0.951$, $p< 0.001$) and with T1 ($r= 0.973$, $p< 0.001$).[62] Feasibility at 3T has also been demonstrated where myocardial T2 values correlated with T2* in a small 8-patient study ($p= 0.93$, $p<0.0001$)[63]

Other potential clinical uses for T2* mapping

Despite the large literature and references to T2* mapping and iron overload assessment, there has been increased interest in applying this technique to other cardiovascular pathologies, especially now given the newer methods with automated maps and free-breathing acquisitions. The first particular area of interest is the ability of T2* to identify changes in myocardial oxygenation and perfusion under stress, a concept first demonstrated in humans as early as 1996 through blood oxygen level dependent (BOLD) imaging using T2*.[64, 65]As vasodilation takes place, the consumption of oxygen is lower due to lower oxygen extraction rates, resulting in a

decrease in the concentration of paramagnetic deoxyhemoglobin and increase in diamagnetic oxyhemoglobin. Therefore, an increase in T2* values is seen under stress, with magnitudes of 10-17%.[66, 67] The ability to detect significant changes in myocardial oxygenation led to the possibility of detection of areas of the myocardium with altered blood oxygen/supply balance in coronary artery disease and adenosine T2* imaging demonstrated a high sensitivity but low specificity in the correlation with angiographically determined stenosis.[68] At 3T, the BOLD effects with T2* are more pronounced given the faster decay ratios that affect the signal intensity and using this field strength other authors have demonstrated more pronounced changes in ΔT2* in patients with normal coronary arteries compared to non-stenotic lesions and severely obstructive disease.[69] The same principle at 3T was also applied showing an increase in T2* in areas of the myocardium perfused by normal coronaries versus no changes in stenotic lesions.[70] The main problems with these studies have been the large number of segments not analyzed because of artifacts, resulting in approximately 25% loss of data. Given the technical developments in T2* mapping sequences, these limitations might be overcome and application of this technique in clinical routine can be applied. Figure 8 shows an example of the T2* maps in a patient with normal coronaries undergoing pharmacological stress test and identifying the vasodilatory effects pre-contrast, with comparative myocardial blood flow images and splenic switch-off confirmation post-contrast.

Another potential use of T2* maps beyond iron overload is in the investigation of microvascular obstruction and intramyocardial hemorrhage. Hemoglobin breakdown, especially in the acute phases of myocardial infarction, leads to areas of signal nulling within infarcted areas which can be appreciated with T2* maps. In a comparison with T2 techniques, T2* proved more sensitive

to detect areas of hemorrhagic infarctions with significant reductions in signal of 54% versus only marginal elevations in remote areas.[71] Given the important prognostic role of both microvascular obstruction and intramyocardial hemorrhage in adverse events and negative left ventricle remodeling, accurate identification and quantification of these phenomena have been an important goal in treating acute CAD patients.[72] Therefore, current evidence suggests that T2* mapping is recommended during the multi-parametric evaluation of patients with acute or recent myocardial infarction.[70] Additionally, Bulluck et al have shown that ST segment-elevation myocardial infarction patients with intra-myocardial hemorrhage had residual myocardial iron at follow-up and this may drive chronic inflammation (high T2 value in the surrounding infarct tissue) which is associated with adverse LV remodeling.[73]

References:

1. Messroghli DR, Moon JC, Ferreira VM, et al. Clinical recommendations for cardiovascular magnetic resonance mapping of T1, T2, T2* and extracellular volume: A consensus statement by the Society for Cardiovascular Magnetic Resonance (SCMR) endorsed by the European Association for Cardiovascular Imaging (EACVI). J Cardiovasc Magn Reson 2017;19(1):75.
2. Anderson LJ, Holden S, Davis B, et al. Cardiovascular T2-star (T2*) magnetic resonance for the early diagnosis of myocardial iron overload. Eur Heart J 2001;22(23):2171-2179.
3. Chavhan GB, Babyn PS, Thomas B, et al. Principles, techniques, and applications of T2*-based MR imaging and its special applications. Radiographics : a review publication of the Radiological Society of North America, Inc 2009;29(5):1433-1449.
4. Baksi AJ, Pennell DJ. T2* imaging of the heart: methods, applications, and outcomes. Topics in magnetic resonance imaging : TMRI 2014;23(1):13-20.
5. Wood JC, Ghugre N. Magnetic resonance imaging assessment of excess iron in thalassemia, sickle cell disease and other iron overload diseases. Hemoglobin 2008;32(1-2):85-96.
6. Gossuin Y, Muller RN, Gillis P. Relaxation induced by ferritin: a better understanding for an improved MRI iron quantification. NMR Biomed 2004;17(7):427-432.
7. Ghugre NR, Enriquez CM, Coates TD, et al. Improved R2* measurements in myocardial iron overload. Journal of magnetic resonance imaging : JMRI 2006;23(1):9-16.
8. Westwood M, Anderson LJ, Firmin DN, et al. A single breath-hold multiecho T2* cardiovascular magnetic resonance technique for diagnosis of myocardial iron overload. Journal of magnetic resonance imaging : JMRI 2003;18(1):33-39.

9. Smith GC, Carpenter JP, He T, et al. Value of black blood T2* cardiovascular magnetic resonance. Journal of Cardiovascular Magnetic Resonance 2011;13(1):21.

10. Tanner MA, He T, Westwood MA, et al. Multi-center validation of the transferability of the magnetic resonance T2* technique for the quantification of tissue iron. Haematologica 2006;91(10):1388-1391.

11. Carpenter JP, He T, Kirk P, et al. On T2* magnetic resonance and cardiac iron. Circulation 2011;123(14):1519-1528.

12. He T, Gatehouse PD, Smith GC, et al. Myocardial T2* measurements in iron-overloaded thalassemia: An in vivo study to investigate optimal methods of quantification. Magnetic resonance in medicine 2008;60(5):1082-1089.

13. Westwood MA, Anderson LJ, Firmin DN, et al. Interscanner reproducibility of cardiovascular magnetic resonance T2* measurements of tissue iron in thalassemia. Journal of magnetic resonance imaging : JMRI 2003;18(5):616-620.

14. Feng Y, He T, Feng M, et al. Improved pixel-by-pixel MRI R2* relaxometry by nonlocal means. Magnetic resonance in medicine 2014;72(1):260-268.

15. Feng Y, He T, Gatehouse PD, et al. Improved MRI R2 * relaxometry of iron-loaded liver with noise correction. Magnetic resonance in medicine 2013;70(6):1765-1774.

16. www.cmrtools.com. 2010; http://www.cmrtools.com/cmrweb/Regulatory.htm. Accessed 12/03/2010, 2010.

17. www.circlecvi.com. 2010; http://www.circlecvi.com/site/regulatory.php. Accessed 12/03/2010, 2010.

18. Mavrogeni S, Bratis K, van Wijk K, et al. The reproducibility of cardiac and liver T2* measurement in thalassemia major using two different software packages. The international journal of cardiovascular imaging 2013.
19. Bacigalupo L, Paparo F, Zefiro D, et al. Comparison between different software programs and post-processing techniques for the MRI quantification of liver iron concentration in thalassemia patients. Radiol Med 2016;121(10):751-762.
20. Fernandes JL, Sampaio EF, Verissimo M, et al. Heart and liver T2 assessment for iron overload using different software programs. Eur Radiol 2011;21(12):2503-2510.
21. Git KA, Fioravante LA, Fernandes JL. An online open-source tool for automated quantification of liver and myocardial iron concentrations by T2* magnetic resonance imaging. Br J Radiol 2015;88(1053):20150269.
22. Messroghli DR, Rudolph A, Abdel-Aty H, et al. An open-source software tool for the generation of relaxation time maps in magnetic resonance imaging. BMC Med Imaging 2010;10:16.
23. Fernandes JL, Fioravante LAB, Verissimo MP, et al. A free software for the calculation of T2* values for iron overload assessment. Acta radiologica 2017;58(6):698-701.
24. Sandino CM, Kellman P, Arai AE, et al. Myocardial T2* mapping: influence of noise on accuracy and precision. Journal of cardiovascular magnetic resonance : official journal of the Society for Cardiovascular Magnetic Resonance 2015;17(1):7.
25. Carpenter JJ-P, He VT, Kirk NP, et al. On T2* Magnetic Resonance and Cardiac Iron. Circulation 2011;123(14):1519-1528.
26. House MJ, Fleming AJ, de Jonge MD, et al. Mapping iron in human heart tissue with synchrotron x-ray fluorescence microscopy and cardiovascular magnetic resonance.

Journal of cardiovascular magnetic resonance : official journal of the Society for Cardiovascular Magnetic Resonance 2014;16(1).

27. Positano V, Meloni A, Santarelli MF, et al. Fast generation of T2* maps in the entire range of clinical interest: application to thalassemia major patients. Computers in biology and medicine 2015;56:200-210.

28. Kellman P, Xue H, Spottiswoode BS, et al. Free-breathing T2* mapping using respiratory motion corrected averaging. Journal of cardiovascular magnetic resonance : official journal of the Society for Cardiovascular Magnetic Resonance 2015;17(1):3.

29. Saiviroonporn P, Viprakasit V, Boonyasirinant T, et al. Comparison of the region-based and pixel-wise methods for cardiac T2* analysis in 50 transfusion-dependent Thai thalassemia patients. Journal of computer assisted tomography 2011;35(3):375-381.

30. Jin N, da Silveira JS, Jolly MP, et al. Free-breathing myocardial T2* mapping using GRE-EPI and automatic non-rigid motion correction. Journal of cardiovascular magnetic resonance : official journal of the Society for Cardiovascular Magnetic Resonance 2015;17:113.

31. Modell B, Khan M, Darlison M, et al. Improved survival of thalassaemia major in the UK and relation to T2* cardiovascular magnetic resonance. J Cardiovasc Magn Reson 2008;10:42.

32. Chouliaras G, Berdoukas V, Ladis V, et al. Impact of magnetic resonance imaging on cardiac mortality in thalassemia major. J Magn Reson Imaging 2011;34(1):56-59.

33. Angelucci E, Barosi G, Camaschella C, et al. Italian Society of Hematology practice guidelines for the management of iron overload in thalassemia major and related disorders. Haematologica 2008;93(5):741-752.

34. Musallam KM, Angastiniotis M, Eleftheriou A, et al. Cross-talk between available guidelines for the management of patients with beta-thalassemia major. Acta Haematol 2013;130(2):64-73.

35. Verissimo MP, Loggetto SR, Fabron Junior A, et al. Brazilian Thalassemia Association protocol for iron chelation therapy in patients under regular transfusion. Revista brasileira de hematologia e hemoterapia 2013;35(6):428-434.

36. Pennell DJ, Udelson JE, Arai AE, et al. Cardiovascular function and treatment in beta-thalassemia major: a consensus statement from the American Heart Association. Circulation 2013;128(3):281-308.

37. Wood JC, Origa R, Agus A, et al. Onset of cardiac iron loading in pediatric patients with thalassemia major. Haematologica 2008;93(6):917-920.

38. Fernandes JL, Fabron A, Jr., Verissimo M. Early cardiac iron overload in children with transfusion-dependent anemias. Haematologica 2009;94(12):1776-1777.

39. Cappellini MD, Cohen A, Eleftheriou A, et al. Iron Overload. *Guidelines for the clinical management of thalassemia*. 2nd rev ed. Nicosia, Cyprus: Thalassemia International Federation; 2008:33-63.

40. Fernandes JL. MRI for Iron Overload in Thalassemia. Hematology/oncology clinics of North America 2018;32(2):277-295.

41. He T, Gatehouse PD, Kirk P, et al. Black-blood T2* technique for myocardial iron measurement in thalassemia. J Magn Reson Imaging 2007;25(6):1205-1209.

42. Positano V, Pepe A, Santarelli MF, et al. Multislice multiecho T2* cardiac magnetic resonance for the detection of heterogeneous myocardial iron distribution in thalassaemia patients. NMR Biomed 2009;22(7):707-715.

43. Positano V, Pepe A, Santarelli MF, et al. Standardized T2* map of normal human heart in vivo to correct T2* segmental artefacts. NMR Biomed 2007;20(6):578-590.

44. Kirk P, Roughton M, Porter JB, et al. Cardiac T2* magnetic resonance for prediction of cardiac complications in thalassemia major. Circulation 2009;120(20):1961-1968.

45. Torlasco C, Cassinerio E, Roghi A, et al. Role of T1 mapping as a complementary tool to T2* for non-invasive cardiac iron overload assessment. PLoS One 2018;13(2):e0192890.

46. Garbowski MW, Carpenter JP, Smith G, et al. Biopsy-based calibration of T2* magnetic resonance for estimation of liver iron concentration and comparison with R2 Ferriscan. J Cardiovasc Magn Reson 2014;16:40.

47. Storey P, Thompson AA, Carqueville CL, et al. R2* imaging of transfusional iron burden at 3T and comparison with 1.5T. J Magn Reson Imaging 2007;25(3):540-547.

48. Messroghli DR, Greiser A, Frohlich M, et al. Optimization and validation of a fully-integrated pulse sequence for modified look-locker inversion-recovery (MOLLI) T1 mapping of the heart. J Magn Reson Imaging 2007;26(4):1081-1086.

49. Messroghli DR, Radjenovic A, Kozerke S, et al. Modified Look-Locker inversion recovery (MOLLI) for high-resolution T1 mapping of the heart. Magn Reson Med 2004;52(1):141-146.

50. Piechnik SK, Ferreira VM, Dall'Armellina E, et al. Shortened Modified Look-Locker Inversion recovery (ShMOLLI) for clinical myocardial T1-mapping at 1.5 and 3 T within a 9 heartbeat breathhold. J Cardiovasc Magn Reson 2010;12:69.

51. Chow K, Flewitt JA, Green JD, et al. Saturation recovery single-shot acquisition (SASHA) for myocardial T(1) mapping. Magn Reson Med 2014;71(6):2082-2095.

52. Abdel-Gadir A, Vorasettakarnkij Y, Ngamkasem H, et al. Ultrafast Magnetic Resonance Imaging for Iron Quantification in Thalassemia Participants in the Developing World: The TIC-TOC Study (Thailand and UK International Collaboration in Thalassaemia Optimising Ultrafast CMR). Circulation 2016;134(5):432-434.

53. Abdel-Gadir A, Treibel T, Moon JC. Myocardial T1 mapping: where are we now and where are we going? Research Reports in Clinical Cardiology 2014:339.

54. Abdel-Gadir A, Berber R, Porter JB, et al. Detection of metallic cobalt and chromium liver deposition following failed hip replacement using T2* and R2 magnetic resonance. J Cardiovasc Magn Reson 2016;18(1):29.

55. Roujol S, Weingartner S, Foppa M, et al. Accuracy, precision, and reproducibility of four T1 mapping sequences: a head-to-head comparison of MOLLI, ShMOLLI, SASHA, and SAPPHIRE. Radiology 2014;272(3):683-689.

56. Wood JC, Otto-Duessel M, Aguilar M, et al. Cardiac iron determines cardiac T2*, T2, and T1 in the gerbil model of iron cardiomyopathy. Circulation 2005;112(4):535-543.

57. Sado DM, Maestrini V, Piechnik SK, et al. Noncontrast myocardial T1 mapping using cardiovascular magnetic resonance for iron overload. J Magn Reson Imaging 2015;41(6):1505-1511.

58. Abdel-Gadir A, Sado D, Murch S, et al. Myocardial iron quantification using T2* and native T1mapping - a 250 patient study. Journal of Cardiovascular Magnetic Resonance 2015;17(1):P312.

59. Alam MH, Auger D, Smith GC, et al. T1 at 1.5T and 3T compared with conventional T2* at 1.5T for cardiac siderosis. J Cardiovasc Magn Reson 2015;17:102.

60. Hanneman K, Nguyen ET, Thavendiranathan P, et al. Quantification of Myocardial Extracellular Volume Fraction with Cardiac MR Imaging in Thalassemia Major. Radiology 2016;279(3):720-730.

61. Radenkovic D, Weingartner S, Ricketts L, et al. T1 mapping in cardiac MRI. Heart Fail Rev 2017;22(4):415-430.

62. Krittayaphong R, Zhang S, Saiviroonporn P, et al. Detection of cardiac iron overload with native magnetic resonance T1 and T2 mapping in patients with thalassemia. Int J Cardiol 2017;248:421-426.

63. Guo H, Au WY, Cheung JS, et al. Myocardial T2 quantitation in patients with iron overload at 3 Tesla. J Magn Reson Imaging 2009;30(2):394-400.

64. Li D, Dhawale P, Rubin PJ, et al. Myocardial signal response to dipyridamole and dobutamine: demonstration of the BOLD effect using a double-echo gradient-echo sequence. Magn Reson Med 1996;36(1):16-20.

65. Friedrich MG, Karamitsos TD. Oxygenation-sensitive cardiovascular magnetic resonance. J Cardiovasc Magn Reson 2013;15:43.

66. Wacker CM, Bock M, Hartlep AW, et al. Changes in myocardial oxygenation and perfusion under pharmacological stress with dipyridamole: assessment using T*2 and T1 measurements. Magn Reson Med 1999;41(4):686-695.

67. Wacker CM, Hartlep AW, Pfleger S, et al. Susceptibility-sensitive magnetic resonance imaging detects human myocardium supplied by a stenotic coronary artery without a contrast agent. J Am Coll Cardiol 2003;41(5):834-840.

68. Friedrich MG, Niendorf T, Schulz-Menger J, et al. Blood oxygen level-dependent magnetic resonance imaging in patients with stress-induced angina. Circulation 2003;108(18):2219-2223.

69. Jahnke C, Manka R, Kozerke S, et al. Cardiovascular magnetic resonance profiling of coronary atherosclerosis: vessel wall remodelling and related myocardial blood flow alterations. European heart journal cardiovascular Imaging 2014;15(12):1400-1410.

70. Manka R, Paetsch I, Schnackenburg B, et al. BOLD cardiovascular magnetic resonance at 3.0 tesla in myocardial ischemia. J Cardiovasc Magn Reson 2010;12:54.

71. Kali A, Tang RL, Kumar A, et al. Detection of acute reperfusion myocardial hemorrhage with cardiac MR imaging: T2 versus T2. Radiology 2013;269(2):387-395.

72. Hamirani YS, Wong A, Kramer CM, et al. Effect of microvascular obstruction and intramyocardial hemorrhage by CMR on LV remodeling and outcomes after myocardial infarction: a systematic review and meta-analysis. JACC Cardiovasc Imaging 2014;7(9):940-952.

73. Bulluck H, Rosmini S, Abdel-Gadir A, et al. Residual Myocardial Iron Following Intramyocardial Hemorrhage During the Convalescent Phase of Reperfused ST-Segment-Elevation Myocardial Infarction and Adverse Left Ventricular Remodeling. Circ Cardiovasc Imaging 2016;9(10).

74. Hansen MS, Sorensen TS. Gadgetron: an open source framework for medical image reconstruction. Magn Reson Med 2013;69(6):1768-1776.

Figures:

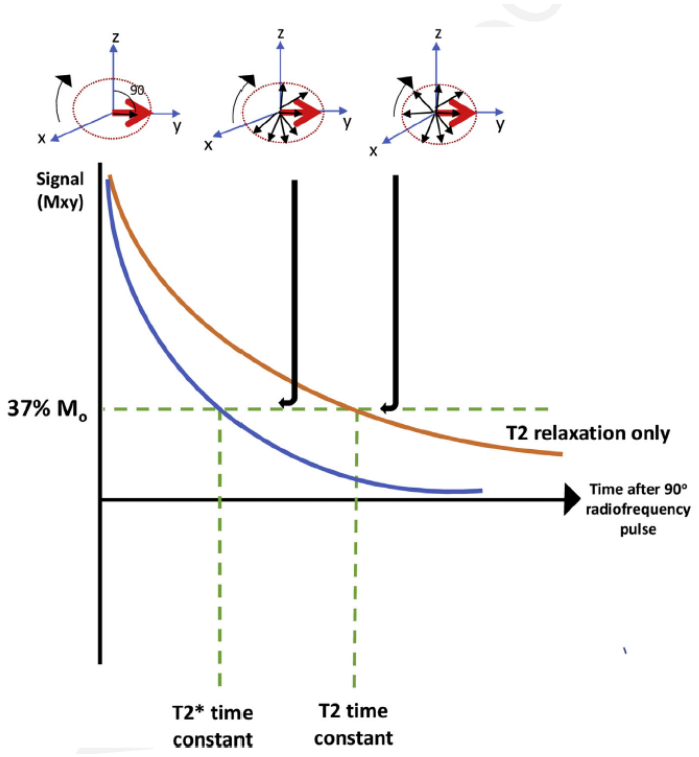

Figure 1: **Schematic illustration of T2* and T2 decay:** Transverse relaxation after an initial 90-degree radiofrequency pulse. A transverse magnetization (small red arrow) has a maximum amplitude as the population of proton magnetic moments (spins) rotate in phase. The amplitude of the net magnetization decays as the proton magnetic moments move out of phase with one another (small black arrows). The overall term for the observed loss of phase coherence (de-phasing) is *T2* relaxation* (which is the combination of T2 relaxation and local variations inhomogeneties in the applied magnetic field). T2 relaxation is the result of spin-spin interactions and this process in irreversible. T2* decay occurs when refocusing pulses are not used and its signal occurs faster (blue curve). Both T2 and T2* are exponential processes with time constants T2 and T2* respectively. This is the time at which the magnetization has decayed to 37% of its initial value after 90 radiofrequency pulse. *Adapted from of John P Ridgway. Cardiovascular magnetic resonance physics for clinicians: part I. Journal of Cardiovascular Magnetic Resonance 2010, 12:71, with permission.*

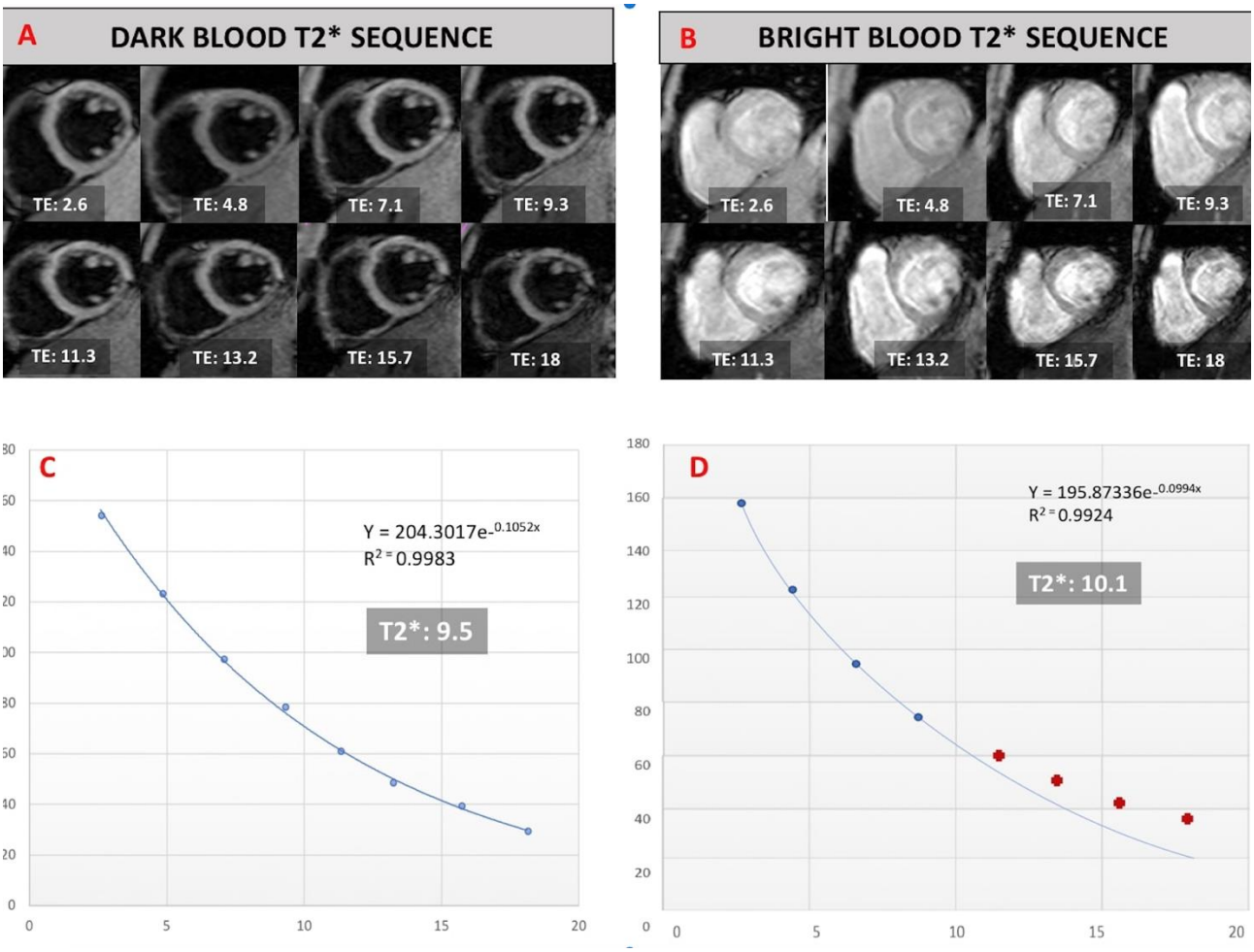

Figure 2: ***A and B:*** Mid ventricular short axis image at different echo time (ET) between 2 to 18 milliseconds (ms), in a patient with beta-thalassemia. Image quality of black –blood sequence is superior (less artifact susceptibility) when compared to bright blood image. ***C:*** Dark blood image analysis - background noise is reduced and curve shows a good fit for the eight gradient echo time without the use of truncation (R^2 = 0.9983, T2* = 9.5ms). This reduces the risk of errors during analysis. ***D:*** Bright blood image analysis – the last four points (red circle) fall below the background noise and are removed to improve the curve fit using the truncation method (R^2 = 0.9924, T2* = 10.1ms).

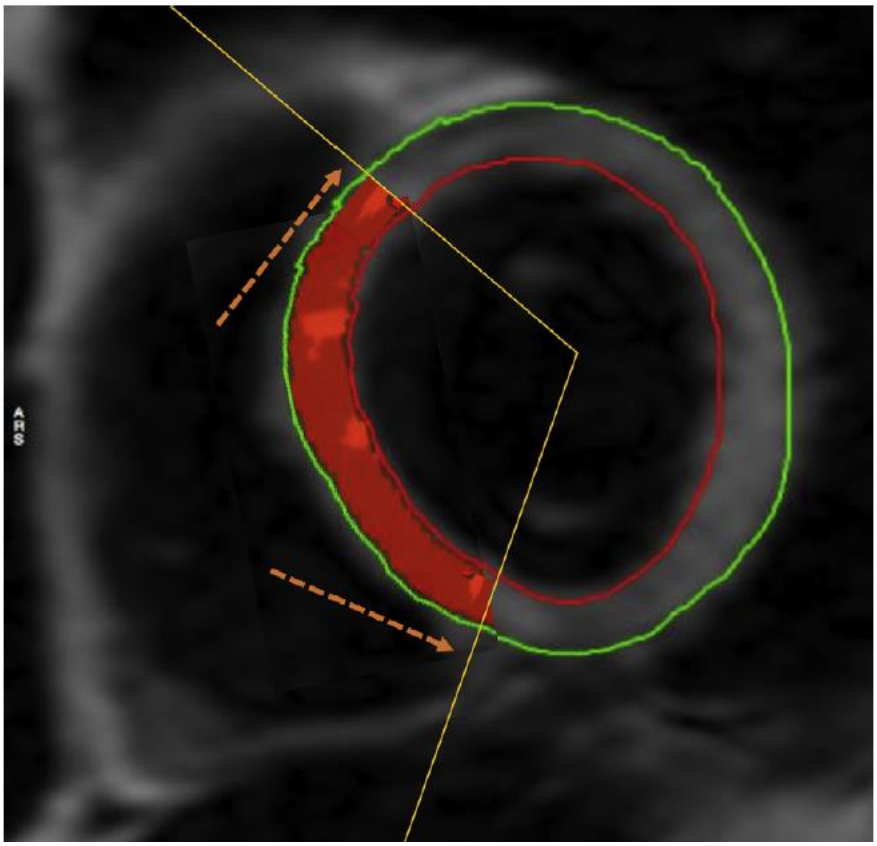

Figure 3: Mid ventricular short axis slice of the heart showing the correct assessment of iron quantification with T2* method: Full-thickness region of interest (ROI) is defined by limiting the epicardial and endocardial border (gradient infiltration starting at epicardium). Analysis is restricted to the septum, in order to avoid artifacts from anterior and posterior cardiac veins and the lung. From Bulluck H, Rosmini S, Abdel-Gadir A, et al. Residual Myocardial Iron Following Intramyocardial Hemorrhage During the Convalescent Phase of Reperfused ST-Segment-Elevation Myocardial Infarction and Adverse Left Ventricular Remodeling. Circ Cardiovasc Imaging 2016;9(10)., with permission.

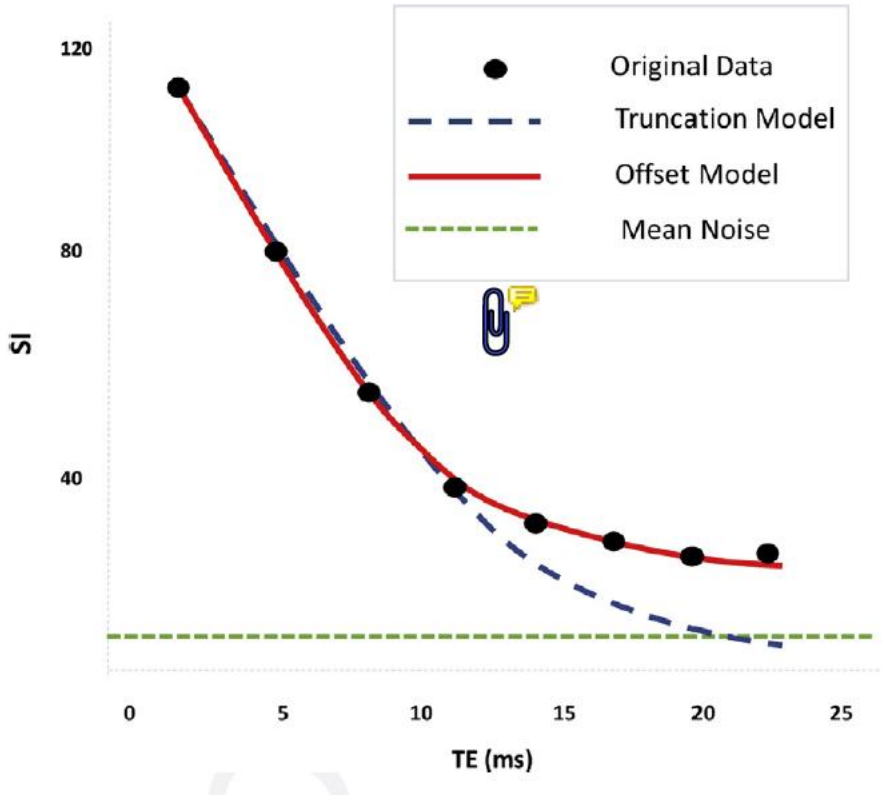

Figure 4: An example showing patient data fitted using both the *offset* and *truncation model*s. The *offset model* fits all the data points well (R2=0.996, T2*=4.4ms, red line) while the *truncation model* fitted the first 4 points only (R2=0.999, T2*=6.9ms, blue dotted line). The mean noise as measured from a background region (green dotted line*). From* Westwood MA, Anderson LJ, Firmin DN, et al. Interscanner reproducibility of cardiovascular magnetic resonance T2* measurements of tissue iron in thalassemia. Journal of magnetic resonance imaging : JMRI 2003;18(5):616-620, with permission.

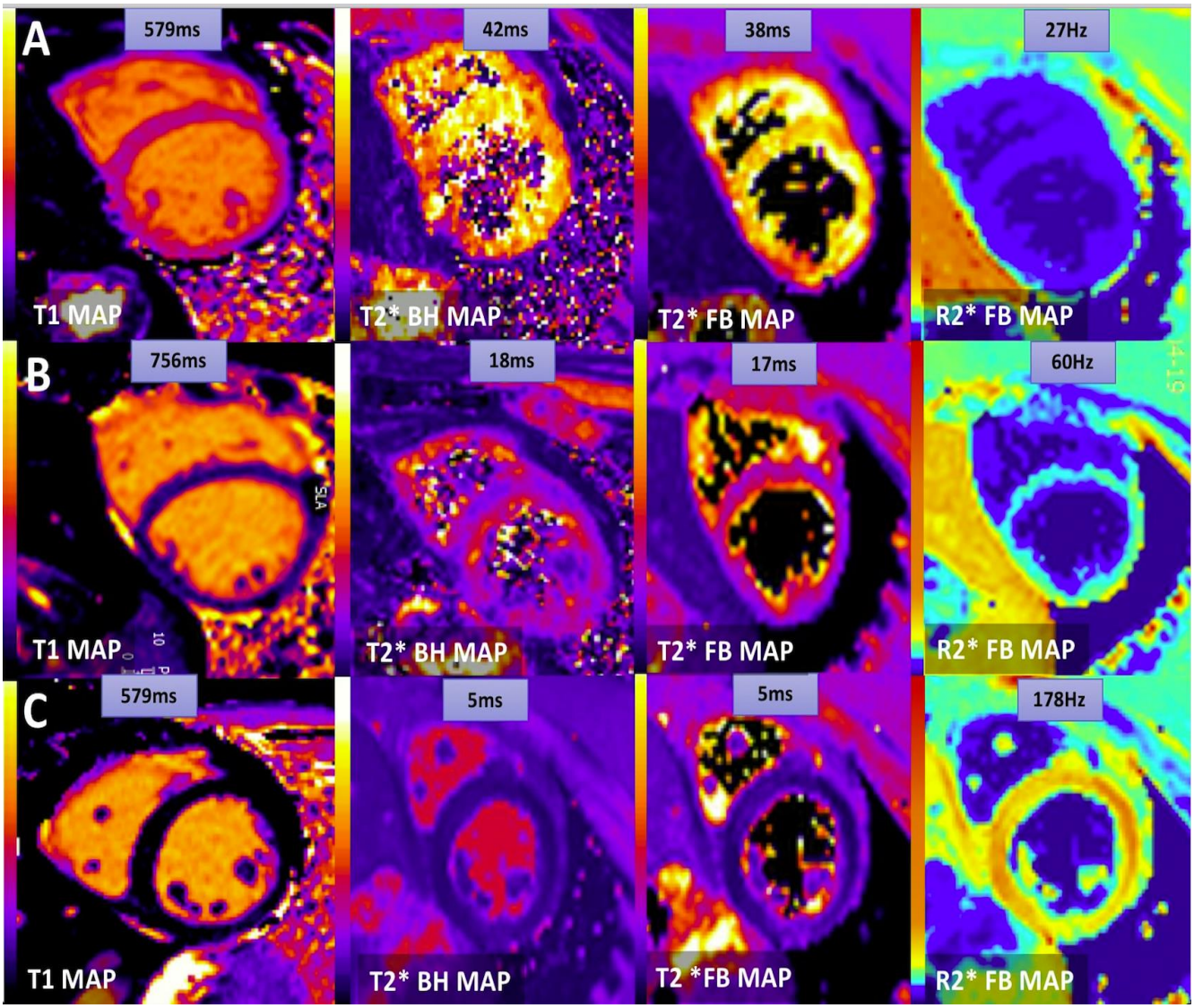

Figure 5: Examples of mappings techniques T1 and T2* in a) a normal patient b) a patient with mild myocardial iron overload and c) a patient with severe liver iron overload. Note that in patients b and c, there is transmural gradient of iron distribution. BH = breath-hold, GB = Free-breathing, ms = milliseconds, Hz = Hertz.

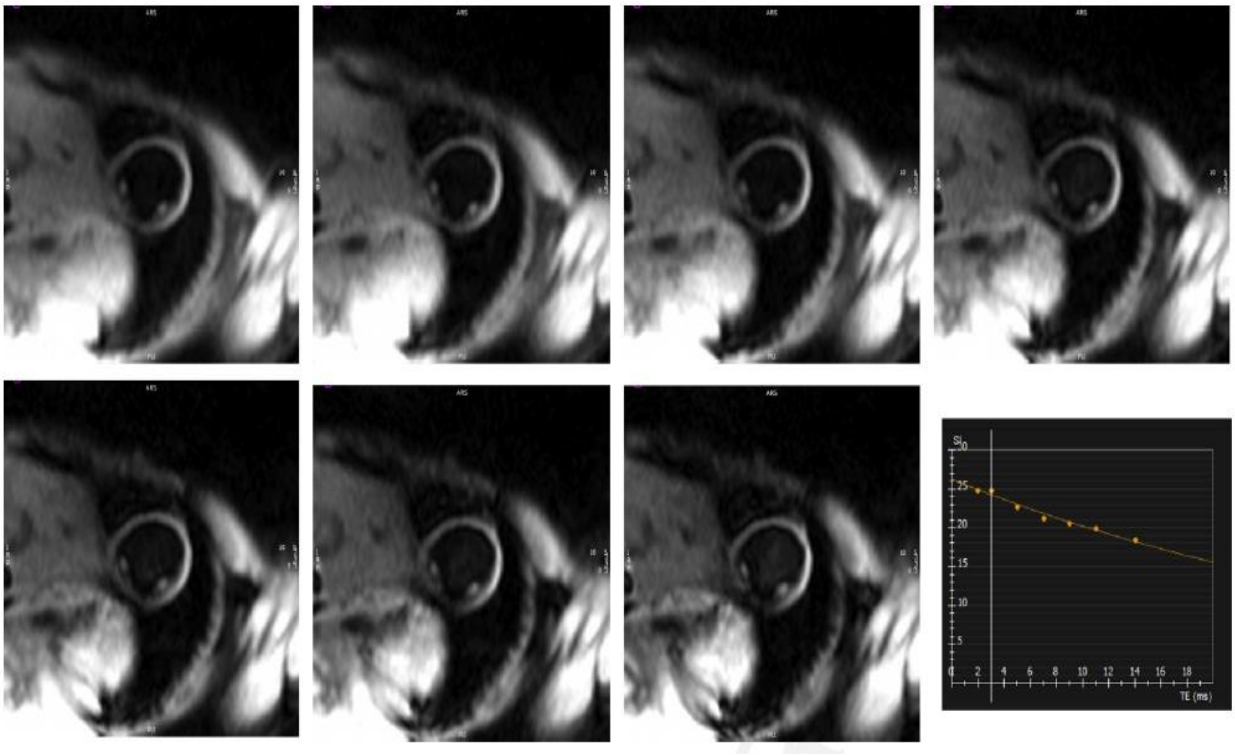

Figure 6: A T2* series of seven images acquired in a 4-year old boy using a free-breathing GRE-EPI sequence with TE varying from 1.97ms to 14.0ms. The corresponding decay curve is shown as well and the calculated T2* was normal at 36.5ms. This series has motion correction already applied and generates clear images of the septum using the black blood technique allowing for accurate placement of a region of interest and T2* calculation. GRE-EPI: gradient-echo, echo-planar imaging; TE: time of echo

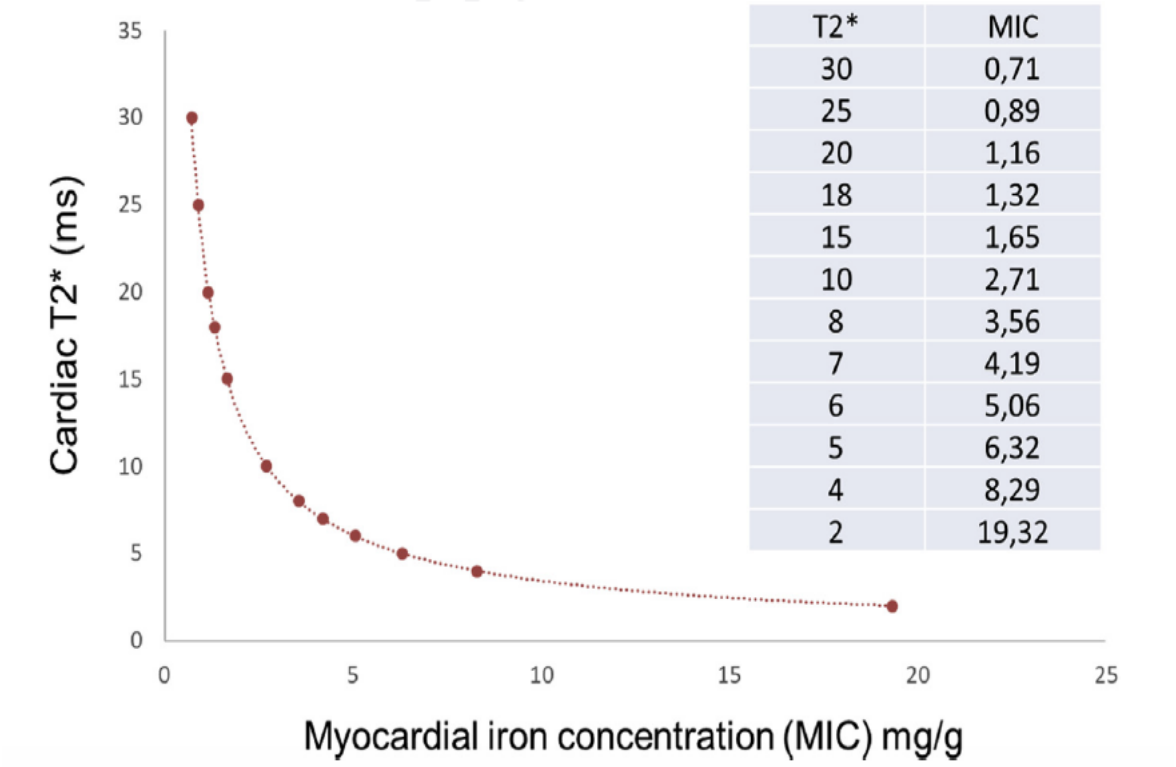

T2*	MIC
30	0,71
25	0,89
20	1,16
18	1,32
15	1,65
10	2,71
8	3,56
7	4,19
6	5,06
5	6,32
4	8,29
2	19,32

Figure 7: Correlation of myocardial T2* and myocardial iron concentration (MIC) with the corresponding curve and some calculated examples. From this graph, it is important to appreciate that changes in T2* above 30ms do not significantly change the final MIC values, whereas small changes in T2* (i.e. below 10ms) significantly increase MIC.

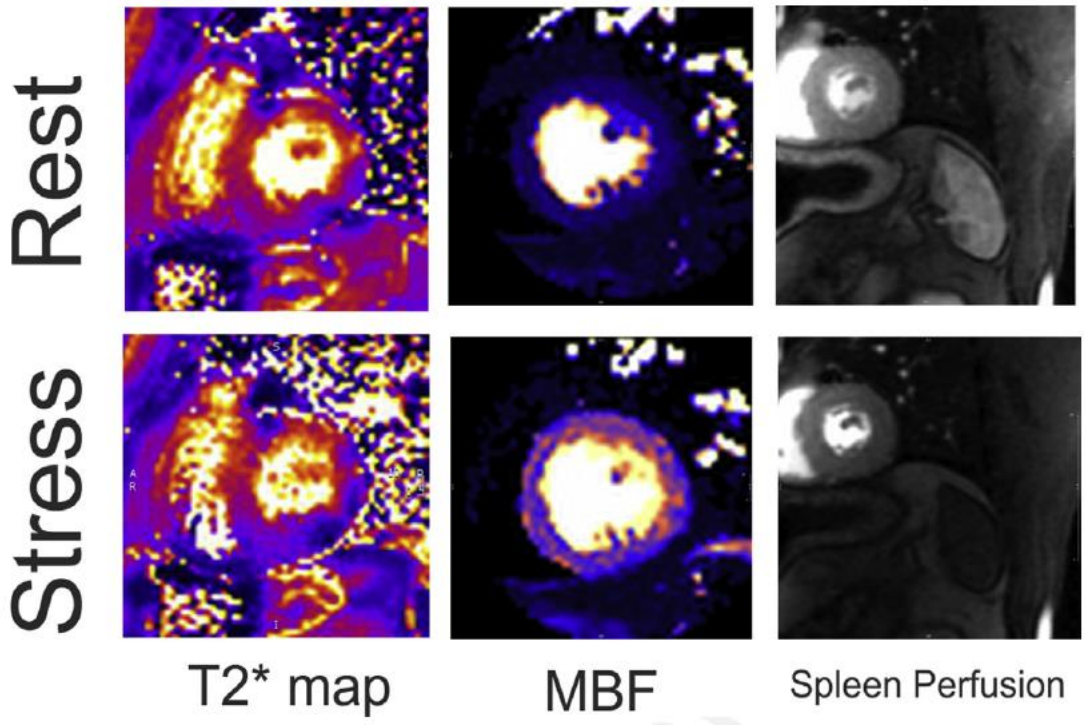

Figure 8: Free-breathing motion-corrected 3T T2* maps, myocardial blood flow (MBF) maps and first-pass perfusion images of the heart/spleen at rest and stress. T2* at rest increased from 21.2ms to 24.4ms (+15.1%) in this patient with normal coronary arteries, with the correlated increase in MBF and splenic-switch off. The T2* maps were obtained prior to any contrast infusion allowing for accurate assessment of a positive vasodilatory induction of dipyridamole prior to injection. Courtesy of Peter Kellman, NIH, USA.

Table 1 – Reference Values for Liver and Myocardial Iron Concentrations for MRI

T2* (ms) 1.5T	R2* (Hz) 1.5T	T2* (ms) 3.0T	R2* (Hz) 3.0T	MIC/LIC (mg/g dw)	Classification
Myocardium					
≥ 20	≤ 50	≥ 12.6	≤ 79	≤ 1.16	Normal
10 to 20	51 to 100	5.8 to 12.6	80 to 172	> 1.16 to 2.71	Mild to Moderate
< 10	> 100	< 5.8	> 172	> 2.71	Severe
Liver					
≥ 15.4	≤ 65	≥ 8.4	≤ 119	≤ 2.0	Normal
4.5 to 15.4	66 to 224	2.3 to 8.4	120 to 435	>2.0 to 7.0	Mild
2.1 to 4.5	225 to 475	1.05 to 2.3	436 to 952	> 7.0 to 15	Moderate
< 2.1	> 475	< 1.05	> 952	> 15	Severe

LIC = liver iron concentration; MIC = myocardial iron concentration; We include T2* and R2* values at 3T but advise caution and recommend normality is defined locally, if 3T has to be used. Data from references 11, 46, 47

Acknowledgements

We thank Dr Peter Kellman (Medical Signal and Image Processing Program; National Heart, Lung, and Blood Institute; NIH, USA) for his valuable comments and suggestions to improve the manuscript and overall support on implementing some of the sequences used in the figures.